

A Mechanistic Interpretation of Syllogistic Reasoning in Auto-Regressive Language Models

Geonhee Kim¹, Marco Valentino³, André Freitas^{1,2,3}

¹ Department of Computer Science, University of Manchester, United Kingdom

² Cancer Biomarker Centre, CRUK Manchester Institute, United Kingdom

³Idiap Research Institute, Switzerland

geonhee.kim@student.manchester.ac.uk

{marco.valentino, andre.freitas}@idiap.ch

Abstract

Recent studies on logical reasoning in auto-regressive Language Models (LMs) have sparked a debate on whether such models can learn systematic reasoning principles during pre-training or merely exploit superficial patterns in the training data. This paper presents a mechanistic interpretation of syllogistic reasoning in LMs to further enhance our understanding of internal dynamics. Specifically, we present a methodology for circuit discovery aimed at disentangling content-independent reasoning mechanisms from world knowledge acquired during pre-training. Through two distinct intervention methods, we uncover a sufficient and necessary circuit involving middle-term suppression that elucidates how LMs transfer information to derive valid conclusions from premises. Furthermore, we investigate how belief biases manifest in syllogistic reasoning, finding evidence of partial contamination from additional attention heads responsible for encoding commonsense and contextualized knowledge. Finally, we explore the generalization of the discovered mechanisms across various syllogistic schemes and model sizes, finding that the identified circuit is sufficient and necessary for all the schemes on which the model achieves high downstream accuracy ($\geq 60\%$). Overall, our findings suggest that LMs indeed learn transferable content-independent reasoning mechanisms, but that, at the same time, such mechanisms do not involve generalisable and abstract logical primitives, being susceptible to contamination by the same world knowledge acquired during pre-training.

Introduction

Transformer-based Language Models (LMs) have led to remarkable results across various natural language processing tasks (Radford et al. 2018, 2019; Brown et al. 2020; OpenAI et al. 2024; Jason et al. 2022; Bubeck et al. 2023). This success has catalyzed research interest in systematically exploring the reasoning capabilities emerging during pre-training (Clark, Tafjord, and Richardson 2020). Recent findings suggest that logical reasoning abilities may emerge in large-scale models (Rae et al. 2022; Kojima et al. 2022; Wei et al. 2022) or through transfer learning on specialized datasets (Betz, Voigt, and Richardson 2021). However, ongoing debates question whether these models apply systematic inference rules or reuse superficial patterns learned during pre-training (Talmor et al. 2020; Kassner, Krojer, and Schütze 2020; Wu et al. 2024). This controversy underscores

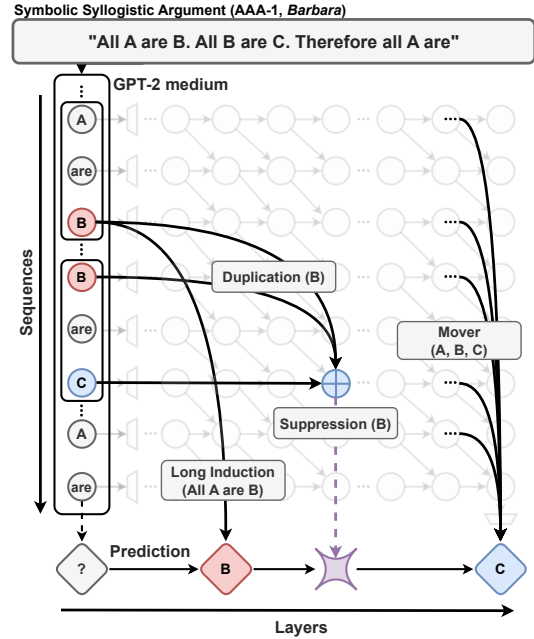


Figure 1: Conceptual representation of the circuit for processing symbolic syllogisms: (Long Induction) Early layers exhibit biases towards the wrong conclusion due to long-range repetition of the first premise “All A are B”. (Duplication) Induction heads aggregate information about duplicated middle terms. (Suppression) The model inhibits middle-term information (i.e., ‘B’), suppressing the long induction mechanism. (Mover) Token-specific information is propagated to the last token position. The process culminates in the prediction shift from ‘B’ to the correct token, ‘C.’

the need for a deeper understanding of the low-level logical inference mechanisms in LMs (Rožanova, Valentino, and Freitas 2024; Rožanova et al. 2023, 2022).

To improve our understanding of the internal mechanisms, this paper focuses on Mechanistic Interpretability (Olah et al. 2020; Nanda et al. 2023), aiming to discover the core circuit responsible for content-independent syllogistic reasoning. In particular, we focus on categorical syl-

logisms with universal affirmative quantifiers (i.e., AAA-1, *Barbara*) motivated by two key factors. First, as observed in natural logic studies (MacCartney and Manning 2007), this form of syllogistic reasoning is prevalent in everyday language. Therefore, it is likely that LMs are exposed to such reasoning schema during pre-training. Second, AAA-1 is a form of unconditionally valid syllogism independent of the premises’ truth condition (Holyoak and Morrison 2005). This characteristic offers a deterministic and scalable task design, other than allowing us to investigate the disentanglement between reasoning and knowledge representation.

Through the adoption of Activation Patching (Meng et al. 2022) and embedding space analysis (i.e., Logit Lens) (Nostalgebraist 2020; Geva et al. 2022; Dar et al. 2023), we investigate the following main research questions: *RQ1: What is the content-independent syllogistic reasoning mechanism internalized in LMs during pre-training?*; *RQ2: Are content-independent mechanisms disentangled from specific world knowledge and belief biases?*; *RQ3: Does the core reasoning mechanism generalize across model sizes and different syllogistic schemes?*

To answer these questions, we present a methodology that consists of 3 main stages. First, we define a syllogistic completion task designed to assess the model’s ability to predict valid conclusions from premises and facilitate the construction of test sets for circuit analysis. Second, we implement a circuit discovery pipeline on the syllogistic schema instantiated only with symbolic variables (Table 1, Symbolic) to identify the core sub-components responsible for content-independent reasoning. We conduct this analysis under two intervention methods: *middle-term corruption* and *all-term corruption*, aiming to identify latent transitive reasoning mechanisms and term-related information flow. Third, we investigate the generalization of the identified circuit on concrete schemes instantiated with commonsense knowledge to identify potential belief biases and explore how the internal behavior varies with different schemes and model sizes.

We present the following overall conclusions:

1. The circuit analysis reveals that auto-regressive LMs develop specific inference mechanisms during pre-training, finding evidence supporting a three-stage mechanism for syllogistic reasoning: (1) naive recitation of the first premise; (2) suppression of duplicated middle-term information; and (3) mediation towards the correct output through the interplay of attention heads.
2. Further experiments on circuit transferability demonstrate that the identified mechanism is still necessary for reasoning on syllogistic schemes instantiated with commonsense knowledge. However, a deeper analysis suggests that specific belief biases acquired during pre-training might play an important role, contaminating the content-independent circuit mechanism with additional attention heads responsible for encoding general and contextualized world knowledge.
3. We found that the identified circuit is sufficient and necessary for all the syllogistic schemes in which the model achieves high downstream accuracy ($\geq 60\%$). This result suggests that LMs learn content-independent reasoning

Premises ($\mathcal{P}_1, \mathcal{P}_2$)	Conclusion (\mathcal{C})
Symbolic All A are B. All B are C.	Therefore, all A are <u>C</u> .
Belief-consistent (True premises) All men are humans. All humans are mortal.	Therefore, all men are mortal .
Belief-inconsistent (False premises) All pilots are people. All people are blond.	Therefore, all pilots are blond .

Table 1: Examples of the same syllogistic schema (i.e., AAA-1, *Barbara*) instantiated with different content (with the expected completion in **bold**). The ability to complete the syllogism is a function of the reasoning schema, independent of the specific instantiation or truth condition of the premises.

mechanisms transferable across abstract schemes.

4. The intervention results on models with different sizes show similar suppression mechanism patterns and information flow. However, we found evidence that the contribution of attention heads becomes more complex with model sizes, further supporting the hypothesis of increasing contamination from external world knowledge.

Our following study is conducted using Transformer-Lens (Nanda and Bloom 2022) on an Nvidia A100 GPU with 80GB of memory. The dataset and code to reproduce our experiments are available online to encourage future work in the field¹.

Methodology

Our main research objective is to discover and interpret the core mechanisms adopted by auto-regressive Language Models (LMs) when performing content-independent syllogistic reasoning. To this end, we present a methodology that consists of 3 main stages. First, we define a syllogistic completion task that can be instrumental for our analysis. Second, we leverage the syllogistic completion task to implement a circuit discovery pipeline on a syllogistic schema instantiated only with symbolic variables (Table 1, Symbolic). Third, we investigate the generalization of the identified circuit on concrete schemes instantiated with commonsense knowledge and explore how the internal behavior varies with different schemes and model sizes.

Syllogism Completion Task

We design a syllogism completion task for assessing the reasoning abilities of LMs, building upon established approaches in the literature (Betz, Voigt, and Richardson 2021; Wu et al. 2023). In particular, we focus on categorical syllogisms with universal affirmative quantifiers (i.e., AAA-1, *Barbara*) because of their frequency in natural language and their content-independent reasoning property.

¹<http://anonymous.url.com>

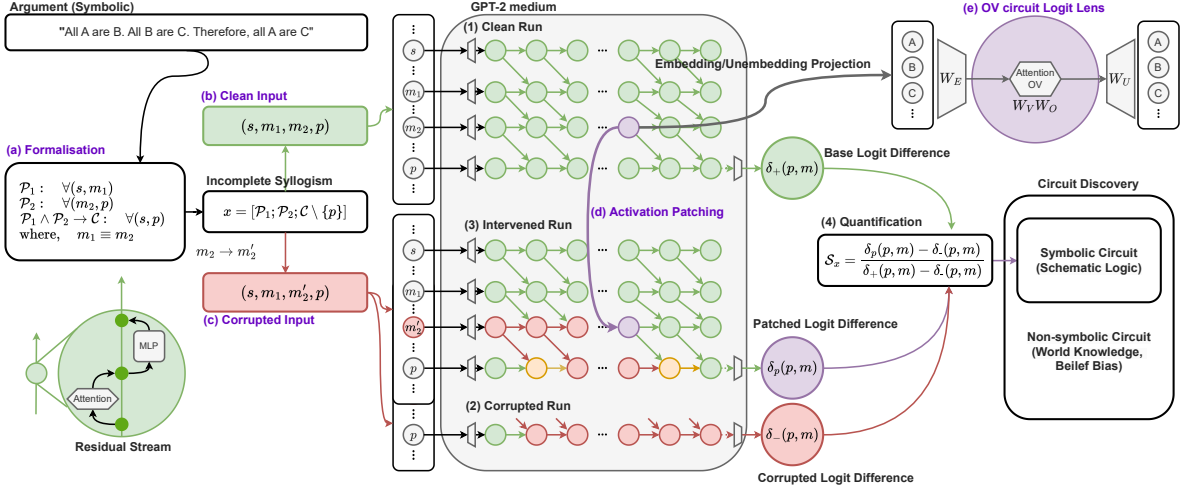


Figure 2: The conceptual pipeline of the symbolic circuit analysis on the syllogism completion task. Figures (a)–(e) illustrate the stages involved in processing a syllogistic argument: argument formalization (a), construction of clean (b) and corrupted inputs (c), activation patching (d) and embedding space analysis (i.e., Logit Lens) (e). The uncovered symbolic circuit is subsequently evaluated to determine whether the core reasoning schema operates independently from world knowledge or belief bias.

The syllogistic argument is typically composed of two premises ($\mathcal{P}_1, \mathcal{P}_2$) and a conclusion (\mathcal{C}), with s and p denoting the subject and predicate terms in the conclusion (e.g. *men* and *mortal*), and m_1 and m_2 (e.g., *humans*) denoting the middle terms in the two premises, with $m_1 \equiv m_2$ in the case of the AAA-1 syllogism.

To evaluate syllogistic reasoning in LMs, we formalize the completion task as masked language modeling, removing the final token p from the conclusion (e.g., *All men are humans. All humans are mortal. Therefore, all men are*), and comparing the probability assigned by the LM to p (e.g., *mortal*) and the middle term m (e.g., *humans*). In general, an LM is successful in the completion of a task if the following condition applies:

$$P(p \mid [\mathcal{P}_1; \mathcal{P}_2; \mathcal{C} \setminus \{p\}]) > P(m \mid [\mathcal{P}_1; \mathcal{P}_2; \mathcal{C} \setminus \{p\}])$$

In our experiments, we measure the logit difference δ between the tokens p and m , defined as $\delta(p, m) = \text{logit}(p) - \text{logit}(m)$, which approximates the log ratio of the conditional probabilities:

$$\delta(p, m) \approx \log \left(\frac{P(p \mid [\mathcal{P}_1; \mathcal{P}_2; \mathcal{C} \setminus \{p\}])}{P(m \mid [\mathcal{P}_1; \mathcal{P}_2; \mathcal{C} \setminus \{p\}])} \right)$$

Dataset Construction. We conduct experiments using two distinct datasets, symbolic and non-symbolic, to derive comparative implications for model reasoning capabilities. The symbolic dataset is constructed by randomly sampling triples (e.g., A, B, and C) from the set of 26 uppercase letters of the English alphabet. On the other side, the non-symbolic dataset is constructed by replacing the letters with words while preserving the syllogistic schema. Here, we generate two different non-symbolic sets: a belief-consistent set containing true premises and a belief-inconsistent set containing false premises (see Table 1). To guarantee the truth condition of the premises, we leverage GenericsKB (Bhaskthavatsalam,

Anastasiades, and Clark 2020), a knowledge base containing statements about commonsense knowledge. The detailed generation process is in Appendix B.

Circuit Discovery

Our main objective is to find a circuit \mathcal{C} for syllogistic reasoning in a Language Model \mathcal{M} . A circuit \mathcal{C} can be defined as a subset of the original model \mathcal{M} that is both sufficient and necessary for achieving the original model performance on the syllogistic completion task. In order to identify a circuit, we employ Activation Patching together with circuit ablation methods (Meng et al. 2022; Vig et al. 2020).

Activation Patching. This technique involves modifying the activation of targeted components and observing the resulting changes. Our study primarily examines the activation of residual streams and multi-head self-attention at the sequence level to trace the term information flow. Given a masked syllogistic input $x = [\mathcal{P}_1; \mathcal{P}_2; \mathcal{C} \setminus \{p\}]$ as (s, m_1, m_2, p) , which can be read as “All s are m_1 . All m_2 are p . Therefore, all s are [mask]”, and its correct completion $y = p$, the Activation Patching technique consists of the following steps:

- (1) **Clean Run:** For the target input (s, m_1, m_2, p) , we record the baseline logit difference, $\delta_+(p, m)$ from the forward pass output of the model (Figure 2(1)).
- (2) **Corrupted Run:** We re-run the model on a corrupted input after applying a specific intervention (e.g., changing the middle term m_2) and record the logit difference $\delta_-(p, m)$ (Figure 2(3)).
- (3) **Intervened Run:** We run the model with the corrupted inputs again and replace the corrupted activations with those from the clean runs to compute the response from the remaining components and measure the causal im-

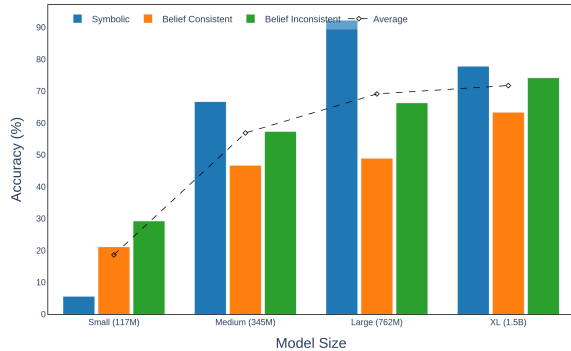


Figure 3: Accuracy on the syllogism completion task across all scales of GPT-2. We observe a phase change from small to medium models in overall performance.

part of the intervention. Here, we measure the adjusted logit difference $\delta_p(p, m)$ (Figure 2(2)).

- (4) **Quantification:** We quantify the causal impact of each intervention using a patching score \mathcal{S} following (Heimersheim and Nanda 2024) as shown in Figure 2(4). This score is further normalized to $[-1, 1]$.

We complement Activation Patching with known methods for analysing hidden activations in transformers, including Logit Lens (Nostalgebraist 2020) with an input-agnostic approach (Dar et al. 2023; Hanna, Liu, and Variengien 2024). Additional technical details can be found in Appendix C.

Interventions. The choice of tokens to corrupt is a critical aspect of the experimental design, and it is essential to establish an appropriate type of intervention that aligns with the hypothesis being tested. In this study, we employ two distinct interventions to isolate the mechanisms related to the reasoning schema from the propagation of specific token information:

- (1) **Middle-Term Corruption:** To investigate the reasoning mechanism employed in the syllogism completion task, we primarily focus on the transitive property of the middle term, $(m_1 \rightarrow m_2) \wedge (m_1 \equiv m_2)$. We hypothesize that disrupting the transitive property will localize the component responsible for syllogistic reasoning. Therefore, our intervention method replaces the second middle term m_2 with an unseen symbol m'_2 , breaking the equality and effectively corrupting the validity of the reasoning, pivoting the correct answer towards m : $(s, m_1, m_2, p) \rightarrow (s, m_1, m'_2, p)$.
- (2) **All-Term Corruption:** We examine how term-related information flows to the last position for the final prediction to identify potential mover heads. To this end, we replace the original terms (s, m_1, m_2, p) with different terms (s', m'_1, m'_2, p') while keeping the completion answers unchanged. We hypothesize that if the mover heads carry the p related information over m related information for a valid prediction, the logit difference will increase; otherwise, it will decrease.

Circuit Ablation. Once we discover a relevant circuit \mathcal{C} , we evaluate its necessity and sufficiency using mean ablation. Specifically, we define a circuit \mathcal{C} as necessary if ablating the identified heads \mathcal{H} in \mathcal{C} and preserving the remaining components in \mathcal{M} decreases the original performance. Conversely, we define a circuit \mathcal{C} as sufficient if preserving only the identified heads \mathcal{H} in \mathcal{C} and ablating all the remaining heads in the original model \mathcal{M} is sufficient to obtain the performance of \mathcal{M} . To perform mean ablation, we gradually average the target attention heads from downstream to upstream layers and measure the average logit difference $\delta(p, m)$ to assess the impact of the ablation on \mathcal{M} . Additional details are included in Appendix D.

Empirical Evaluation

Model Selection. We select the LM for the circuit analysis based on a trade-off between model size and performance. To this end, we measure the accuracy of GPT-2 (Radford et al. 2019) with different sizes (117M, 345M, 762M, and 1.5B) on the syllogism completion task. Specifically, we aim to identify potential phase transition points where significant performance changes emerge (Jason et al. 2022; Kaplan et al. 2020). As shown in Figure 3, we observe a notable phase transition from small to medium sizes, where average performance increases by 139.97% in the symbolic setting and 119.21% in the non-symbolic setting. Given these results, we select *GPT-2 Medium* for circuit discovery and subsequently test the compatibility with different model sizes (See Appendix E for the model architecture). For all experiments, we use 90 samples each for symbolic and non-symbolic arguments to balance the depth of analysis with computational efficiency.

Localization of Transitive Reasoning Mechanisms

Middle-term corruption reveals information flow relevant to the transitive property. Figure 4(a-b) presents the results of the middle-term intervention targeting attention heads and residual stream. Figure 4(a), in particular, reveals the positive role of heads $\mathbf{h}_{11.10}$ and $\mathbf{h}_{19.1}$ (where $\mathbf{h}_{l.k}$ denotes the k th head in layer l). Moreover, we observe an information propagation pattern from the $[m_2]$ position to the $[p]$ position (Figure 4(b)). These observations allow us to hypothesize that information from $[m_2]$ is conveyed to $[p]$ on the residual stream by attention head $\mathbf{h}_{11.10}$, which exhibits a strong patching score around the layer responsible for the propagation. To verify this hypothesis, we further investigate the attention weights between $[p]$ and $[m_2]$. As expected, $[m_2]$ is the position most highly attended by $[p]$, with an average attention weight of 0.15 ± 0.07 (Figure 4(e)). These results suggest that information is indeed moved from $[m_2]$ to $[p]$ on the residual stream subspace, with $\mathbf{h}_{11.10}$ playing a crucial role in this mechanism.

Duplicate middle-term information is aggregated via induction heads. We further investigate how information from $[m_2]$ is moved to $[p]$, positing that this relates to the model’s internal reasoning mechanism. We notice that at position $[p]$, the model can observe the complete AAA-1

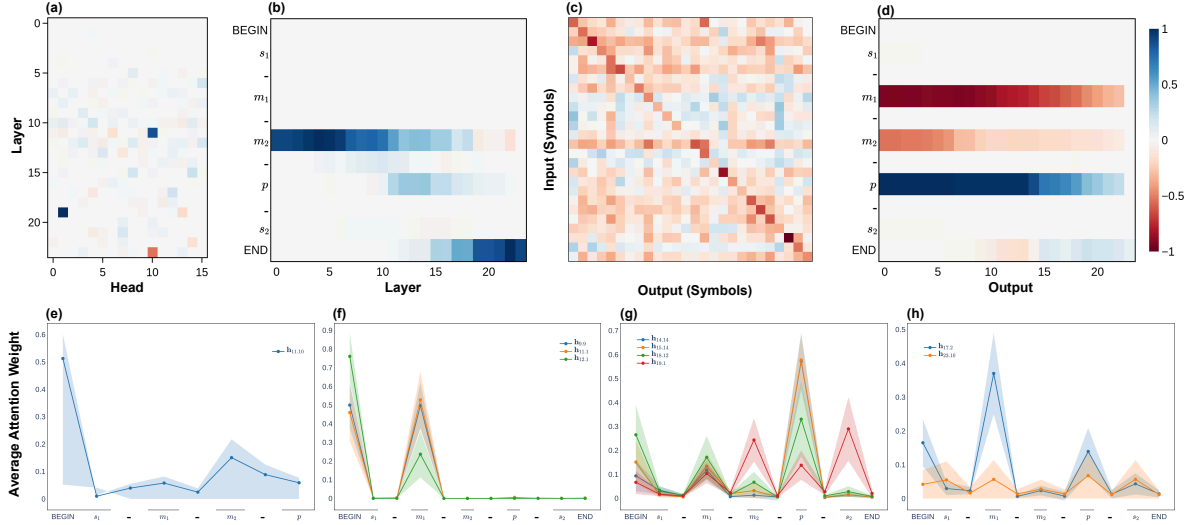


Figure 4: Comprehensive results of the symbolic circuit analysis. (a) Attention output patching results and (b) residual stream patching results in the middle-term intervention setup. (c) OV circuit logit lens results for $h_{11.10}$, with input and output comprising 26 uppercase letters. (d) Residual stream patching results in the all-term corruption setup. (e)-(h) Average attention patching weights across the batch: (e) weights for token position $[p]$ attending, and (f)-(h) weights for the last token position attending. For clarity, the y-axis legend denotes tokens appearing between terms, separated by a ‘-’ symbol, with averaged values.

syllogistic structure (Figure 2(a)) with middle-term duplication. We hypothesize that this structural information for reasoning is collected at one position, given that information refinement occurs at the specific position such as last token (Hanna, Liu, and Variengien 2024; Stolfo, Belinkov, and Sachan 2023). To verify this, we trace the information flow of head $h_{11.10}$ using path patching (Wang et al. 2023). Our results show that $h_{11.10}$ operates based on several induction heads (Elhage et al. 2021) ($h_{5.8}$, $h_{6.1}$, $h_{6.15}$ and $h_{7.2}$) formed at $[m_2]$. These heads attend to the $[[m_1] + 1]$ token due to the $m_1 \equiv m_2$ conditioned matching operation, likely containing m_1 -related information from previous token heads. We conclude, therefore, that m_1 and m_2 information are aggregated at position $[p]$. Additional details of the path patching results are available in the Appendix F.

Suppressive mechanism is revealed through Logit Lens.

To better understand the internal mechanism occurring at the $[p]$ position, we investigate attention head $h_{11.10}$. Having previously examined the attention pattern (composed of attention weights), we now focus on the attention value and output by analyzing the OV circuit ($W_V W_O$) (Elhage et al. 2021) using the logit lens method (Nostalgebraist 2020). Interestingly, the result in Figure 4(c) shows a clear negative diagonal pattern suggesting that $h_{11.10}$ strongly suppresses the logit when attending to the same token as the corresponding output. Given our previous findings that $h_{11.10}$ reads information from the subspace of token $[m_2]$, we conclude that it applies a suppressive mechanism to m -related information and writes it back to the residual stream’s subspace at $[p]$. If later heads carry this information to the last token, this mechanism becomes crucial for the model to arrive at the correct answer. For simplicity, we name head

$h_{11.10}$ as m -suppression head.

Localization of Term-Related Information Flow

Key information is moved from term-specific positions to the last position. Now, we use the all-term intervention method to localize mover heads that carry term-related information. In the residual stream patching results (Figure 4(d)), we observe the highest positive score at the $[p]$ position, while negative scores are most prominent at the $[m_1]$ and $[m_2]$ positions, indicating that the information residing in these positions indeed contributes to their corresponding token prediction. This observation aligns with the importance of token embedding information at their respective positions given iterative refinement on the residual stream (Simoulin and Crabbé 2021). A closer examination of the last token position reveals that the negative effect propagates from relatively early layers (approximately layer 10 onwards), yet positive effects are from later layers (approximately layer 14 onwards), incurring a positive shift of the model’s prediction from m to p .

Information is carried by later positive and negative mover heads.

Given the findings that the information for prediction resides in term-specific positions, we trace which attention heads transfer the information from each term position ($[p]$, $[m_1]$ and $[m_2]$) to the last token. We call these heads mover heads as the existence of “positive or negative mover heads” that carry or suppress information from the specific token position to the last token position (Wang et al. 2023; García-Carrasco, Maté, and Carlos Trujillo 2024). To discover the source of information flow, we investigate the heads with high attention value weight (W_V) patching score and identify 9 notable mover heads (see Appendix G for

details of mover heads localization). By further investigation of attention patterns (Figure 4(f)–(h)), $\mathbf{h}_{14.14}$, $\mathbf{h}_{15.14}$ and $\mathbf{h}_{18.12}$ are classified as positive copy heads attending highly to $[p]$, and $\mathbf{h}_{19.1}$ is a positive suppression head by attending to $[m_2]$ and $[s]$. $\mathbf{h}_{9.9}$, $\mathbf{h}_{11.1}$, $\mathbf{h}_{12.1}$, $\mathbf{h}_{17.2}$ and $\mathbf{h}_{23.10}$ are negative copy heads giving a strong attention to non- $[p]$.

A long induction mechanism in early layer movers causes biases towards the middle term. Notably, the early negative mover heads ($\mathbf{h}_{9.9}$, $\mathbf{h}_{11.11}$ and $\mathbf{h}_{12.1}$ in Figure 4(f)) exhibit significantly high attention to $[m_1]$. This pattern indicates that these heads transfer information from the $[m_1]$ position directly to the last token position, negatively affecting the final prediction and biasing the model towards m . We notice that this behavior closely resembles that of induction heads (Elhage et al. 2021) defined on bi-grams ($[s][are]$) rather than uni-gram ($[are]$), supported by previous token heads in upstream layers (e.g., $\mathbf{h}_{8.1}$).

Summary

Overall, we found that the internal mechanisms to arrive at the correct conclusion involve the following phases:

1. **Long Induction:** Early layers exhibit biases towards the wrong conclusion due to long-range repetition of the first premise “All A are B”.
2. **Duplication:** Induction heads aggregate information about duplicated middle terms in the premises.
3. **Suppression:** The model aggregates and inhibits middle-term information (i.e., “B”) suppressing the long induction mechanism.
4. **Mover:** Token-specific information is propagated to the last token position. The process culminates in the prediction shift from B’ to the correct token ‘C’.

Therefore, **the discovered circuit is mainly characterized by an internal error correction mechanism.** Interestingly, this mechanism is different from the way humans would reason on syllogistic arguments through the use of abstract logical primitives and inference rules.

Circuit Evaluation

To evaluate the comprehensive correctness of the circuit, we assess necessity and sufficiency via the ablation method described in section 2. The ablation study in Figure 5(a) shows that **the identified circuit is both necessary and sufficient**, demonstrating a consistent performance degradation when removing circuit components and revealing a complete restoration of the original model’s performance when considering only the circuit’s subcomponents. We further verify the robustness of the symbolic circuit to superficial and semantic-preserving perturbations. In particular, we modify the letters into numbers (Figure 5(b)) and adopt semantically equivalent quantifiers and related verbs (e.g., “All ... are” is converted into “Each ... is”). The ablation result demonstrates that both types of **perturbations do not undermine the sufficiency and necessity property of the circuit.**

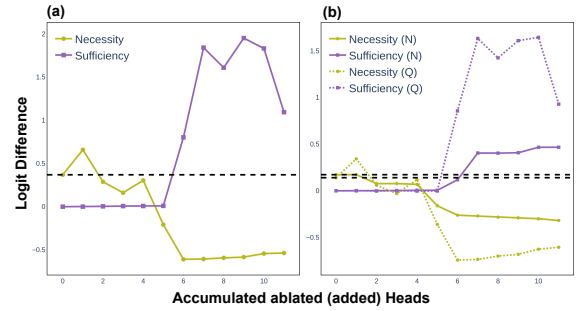


Figure 5: Circuit ablation results for (a) correctness and (b) robustness on the symbolic dataset. Solid lines show numeric perturbation-based performance, dotted lines indicate quantifier perturbation-based performance in (b), and the dashed line shows the baseline logit difference without knockouts.

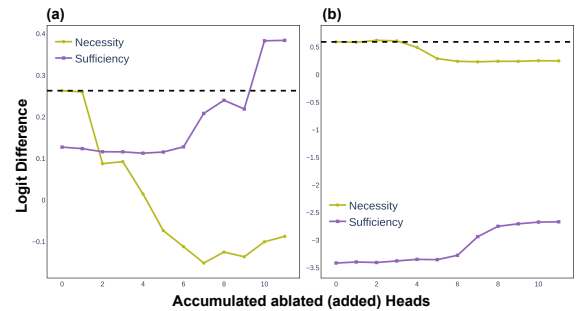


Figure 6: Circuit ablation results for evaluating transferability on non-symbolic datasets: the belief-consistent (a) and the belief-inconsistent (b). The dashed line represents the baseline logit difference without knockouts.

Circuit Transferability

The circuit is necessary for non-symbolic syllogistic arguments, yet not sufficient for belief-inconsistent ones.

We present ablation results for the two generated non-symbolic datasets: belief-consistent (Figure 6(a)) and belief-inconsistent (Figure 6(b)) (See Appendix H for the intervention results). Notably, the symbolic circuit proves necessary for both types of non-symbolic inputs, suggesting that the logic derived from symbolic syllogisms remains essential even when natural words are substituted. Regarding sufficiency, while belief-consistent data show significant performance recovery, we observe an inability to restore original performance on the belief-inconsistent set despite an increasing trend. These results indicate that belief biases encoded in different attention heads may play an important role.

Belief biases corrupt reasoning mechanisms. To further investigate the impact of belief biases, we again conduct intervention experiments. Specifically, we observe that in the AAA-1 syllogism schema (s, m_1, m_2, p) , the subject token s should be irrelevant for deriving the correct answer p over m . Therefore, we leverage this property to verify whether

Mood-Figure	C1	C2	C3	Acc
AII-3 (<i>Datisi</i>)	✓	✓	✓	0.84
IAI-3 (<i>Disamis</i>)	✓	✓	✓	0.68
IAI-4 (<i>Dimaris</i>)	✓	✓	✓	0.68
AAA-1 (<i>Barbara</i>)	✓	✓	✓	0.67
EAE-1 (<i>Celarent</i>)	✓	-	✓	0.59
EIO-4 (<i>Fresison</i>)	✓	-	✓	0.53
EIO-3 (<i>Ferison</i>)	✓	-	✓	0.53
AII-1 (<i>Darii</i>)	✓	✓	-	0.43
AOO-2 (<i>Baroco</i>)	-	-	-	0.24
AEE-4 (<i>Camenes</i>)	-	-	-	0.24
OAO-3 (<i>Bocardo</i>)	✓	-	-	0.22
EIO-1 (<i>Ferio</i>)	✓	-	-	0.18
EIO-2 (<i>Festino</i>)	-	-	-	0.09
EAE-2 (<i>Cesare</i>)	-	-	-	0.08
AEE-2 (<i>Camestres</i>)	-	-	-	0.04

Table 2: Generalizability across unconditionally valid syllogistic forms. Columns C1, C2, and C3 indicate whether conditions are met (✓) or not (-): C1: Necessity, C2: Sufficiency, C3: Positive Logit Difference. ‘Accuracy (Acc)’ shows performance on the completion task for each syllogism.

word-specific biases are introduced when instantiating the schema with concrete knowledge. To this end, we perform Activation Patching by corrupting the subject term, transforming (s, m_1, m_2, p) to (s', m_1, m_2, p) , and measuring the degradation in logit difference as $\delta_+(p, m) - \delta_-(p, m)$. Notably, the non-symbolic setting exhibits a significant performance degradation of 0.66 ± 1.27 , representing a 299.96% change from the baseline. In contrast, the symbolic setting shows a minimal degradation of 0.00 ± 0.64 , a mere 0.35% drop. This drastic difference supports our hypothesis that the knowledge acquired during pre-training corrupts the content-independent reasoning circuit identified on the symbolic set with additional attention heads.

Generalization to Different Syllogistic Schemes

We further aim to understand whether the symbolic circuit is specific to the AAA-1 syllogism (*Barbara*). To this end, we extend our experiment to encompass all 15 unconditionally valid syllogisms (see Appendix A and I for details about the syllogistic schemes and more experimental results). To evaluate the transferability to all 15 schemes, we verify three main conditions, reported in Table 2: (C1) Necessity, (2) Sufficiency, and (C3) Positive Logit Difference. We also measure the accuracy of the completion task for each syllogism. From Table 2, we observe that **the circuit is sufficient and necessary for all the syllogistic schemes in which the model achieves high downstream accuracy ($\geq 60\%$)**, supporting the conclusion that the circuit includes components that are crucial for the emergence of syllogistic reasoning in general. Notably, all three conditions are satisfied for the affirmative syllogisms (AII-3, IAI-3, IAI-4), for which the model achieves an accuracy above 0.6.

Generalization to Different Model Sizes

Finally, we expand our analysis to different sizes of GPT-2 (small, large and XL), assuming core mechanisms would transfer across models trained on the same dataset. Here, **the intervention results show similar suppression mechanism patterns and information flow across all models**. However, the residual stream of GPT-2 small in the all-term corruption setup is reversed due to its low downstream accuracy (see Appendix J). Moreover, **as the model size increases, we found evidence that the contribution of attention heads becomes more complex**. We hypothesize this might be caused by a stronger impact of world knowledge with increasing size, as suggested by the decrease in accuracy on the symbolic dataset and the increase on the non-symbolic set observed for the XL model (See Figure 3).

Related Work

Mechanistic circuit analysis has emerged as a promising approach to interpreting the internal mechanisms of Transformers (Olah et al. 2020; Nanda et al. 2023; Olsson et al. 2022; Wang et al. 2023; García-Carrasco, Maté, and Carlos Trujillo 2024; Hanna, Liu, and Variengien 2024). Existing approaches investigating internal reasoning mechanisms mainly focus on math-related tasks, elucidating the information flow for answering mathematical questions (Stolfo, Belinkov, and Sachan 2023) and examining arithmetic operations (Quirke and Barez 2024). Most pertinent to our work, Wiegrefe et al. (2024) provides a mechanistic interpretation of multiple-choice question answering, investigating attention head-level patterns. In general, our mechanistic analysis complements recent work investigating the challenges in processing reasoning arguments that contradict established beliefs and whether the reasoning in LMs stems from internalized rules or memorized content (Ando et al. 2023; Yu, Merullo, and Pavlick 2023; Wu et al. 2024; Talmor et al. 2020; Wu et al. 2024; Kassner, Krojer, and Schütze 2020; Haviv et al. 2023; Feldman 2020; Monea et al. 2024; Yu, Merullo, and Pavlick 2023; Wallat, Singh, and Anand 2020; Eisape et al. 2024). To address this question, different mechanistic approaches have been adopted to localizing factual associations (Meng et al. 2022; Geva et al. 2023; Dai et al. 2022) or assessing conditions for generalisation (Wang et al. 2024). However, to the best of our knowledge, we are the first to investigate content-independent mechanisms for syllogistic reasoning.

Conclusion

In this study, we have provided a comprehensive mechanistic interpretation of syllogistic reasoning within autoregressive language models. Overall, our findings suggest that LMs indeed learn transferable content-independent reasoning mechanisms but that, at the same time, such mechanisms might be contaminated and suppressed by the same specific world knowledge acquired during pre-training.

It is important to acknowledge some of the limitations in our study: (1) our analysis is conducted predominantly on the transitive property and term-specific information and

does not consider the full spectrum of the reasoning dynamics that might appear in more complex scenarios. (2) Our experimentation is confined to a specific reasoning template that lacks the complexity and noise of real-world problems due to the intricate level of granularity and the computational complexity required in circuit analysis. Despite these limitations, we believe our findings could offer valuable insights into the reasoning mechanisms adopted by autoregressive language models and lay a solid foundation for future research in this field.

Acknowledgements

This work was partially funded by the Swiss National Science Foundation (SNSF) project NeuMath: Neural Discourse Inference over Mathematical Texts (200021_204617).

References

- Ando, R.; Morishita, T.; Abe, H.; Mineshima, K.; and Okada, M. 2023. Evaluating Large Language Models with NeuBAROCO: Syllogistic Reasoning Ability and Human-like Biases. In *Proceedings of the 4th Natural Logic Meets Machine Learning Workshop*, 1–11. Association for Computational Linguistics.
- Betz, G.; Voigt, C.; and Richardson, K. 2021. Critical Thinking for Language Models. In Zarrieß, S.; Bos, J.; van Noord, R.; and Abzianidze, L., eds., *Proceedings of the 14th International Conference on Computational Semantics (IWCS)*, 63–75. Groningen, The Netherlands (online): Association for Computational Linguistics.
- Bhaskthavatsalam, S.; Anastasiades, C.; and Clark, P. 2020. GenericsKB: A Knowledge Base of Generic Statements. arXiv:2005.00660.
- Brown, T.; Mann, B.; Ryder, N.; Subbiah, M.; Kaplan, J. D.; Dhariwal, P.; Neelakantan, A.; Shyam, P.; Sastry, G.; and Askell, A. 2020. Language models are few-shot learners. *Advances in neural information processing systems*, 33: 1877–1901.
- Bubeck, S.; Chandrasekaran, V.; Eldan, R.; Gehrke, J.; Horvitz, E.; Kamar, E.; Lee, P.; Lee, Y. T.; Li, Y.; Lundberg, S.; Nori, H.; Palangi, H.; Ribeiro, M. T.; and Zhang, Y. 2023. Sparks of Artificial General Intelligence: Early experiments with GPT-4. arXiv:2303.12712.
- Clark, P.; Tafjord, O.; and Richardson, K. 2020. Transformers as Soft Reasoners over Language. In Bessiere, C., ed., *Proceedings of the Twenty-Ninth International Joint Conference on Artificial Intelligence, IJCAI-20*, 3882–3890. International Joint Conferences on Artificial Intelligence Organization. Main track.
- Dai, D.; Dong, L.; Hao, Y.; Sui, Z.; Chang, B.; and Wei, F. 2022. Knowledge Neurons in Pretrained Transformers. In Muresan, S.; Nakov, P.; and Villavicencio, A., eds., *Proceedings of the 60th Annual Meeting of the Association for Computational Linguistics (Volume 1: Long Papers)*, 8493–8502. Dublin, Ireland: Association for Computational Linguistics.
- Dar, G.; Geva, M.; Gupta, A.; and Berant, J. 2023. Analyzing Transformers in Embedding Space. In Rogers, A.; Boyd-Graber, J.; and Okazaki, N., eds., *Proceedings of the 61st Annual Meeting of the Association for Computational Linguistics (Volume 1: Long Papers)*, 16124–16170. Toronto, Canada: Association for Computational Linguistics.
- Eisape, T.; Tessler, M.; Dasgupta, I.; Sha, F.; Steenkiste, S.; and Linzen, T. 2024. A Systematic Comparison of Syllogistic Reasoning in Humans and Language Models. In Duh, K.; Gomez, H.; and Bethard, S., eds., *Proceedings of the 2024 Conference of the North American Chapter of the Association for Computational Linguistics: Human Language Technologies (Volume 1: Long Papers)*, 8425–8444. Mexico City, Mexico: Association for Computational Linguistics.
- Elhage, N.; Nanda, N.; Olsson, C.; Henighan, T.; Joseph, N.; Mann, B.; Askell, A.; Bai, Y.; Chen, A.; Conerly, T.; DasSarma, N.; Drain, D.; Ganguli, D.; Hatfield-Dodds, Z.; Hernandez, D.; Jones, A.; Kernion, J.; Lovitt, L.; Ndousse, K.; Amodei, D.; Brown, T.; Clark, J.; Kaplan, J.; McCandlish, S.; and Olah, C. 2021. A Mathematical Framework for Transformer Circuits. *Transformer Circuits Thread*. <https://transformer-circuits.pub/2021/framework/index.html>.
- Feldman, V. 2020. Does learning require memorization? a short tale about a long tail. In *Proceedings of the 52nd Annual ACM SIGACT Symposium on Theory of Computing, STOC 2020*, 954–959. New York, NY, USA: Association for Computing Machinery. ISBN 9781450369794.
- García-Carrasco, J.; Maté, A.; and Carlos Trujillo, J. 2024. How does GPT-2 Predict Acronyms? Extracting and Understanding a Circuit via Mechanistic Interpretability. In Dasgupta, S.; Mandt, S.; and Li, Y., eds., *Proceedings of The 27th International Conference on Artificial Intelligence and Statistics*, volume 238 of *Proceedings of Machine Learning Research*, 3322–3330. PMLR.
- Geva, M.; Bastings, J.; Filippova, K.; and Globerson, A. 2023. Dissecting Recall of Factual Associations in Autoregressive Language Models. In *Proceedings of the 2023 Conference on Empirical Methods in Natural Language Processing*, 12216–12235.
- Geva, M.; Caciularu, A.; Wang, K.; and Goldberg, Y. 2022. Transformer Feed-Forward Layers Build Predictions by Promoting Concepts in the Vocabulary Space. In Goldberg, Y.; Kozareva, Z.; and Zhang, Y., eds., *Proceedings of the 2022 Conference on Empirical Methods in Natural Language Processing*, 30–45. Abu Dhabi, United Arab Emirates: Association for Computational Linguistics.
- Hanna, M.; Liu, O.; and Variengien, A. 2024. How does gpt-2 compute greater-than?: Interpreting mathematical abilities in a pre-trained language model. *Advances in Neural Information Processing Systems*, 36.
- Haviv, A.; Cohen, I.; Gidron, J.; Schuster, R.; Goldberg, Y.; and Geva, M. 2023. Understanding Transformer Memorization Recall Through Idioms. In Vlachos, A.; and Augenstein, I., eds., *Proceedings of the 17th Conference of the European Chapter of the Association for Computational Linguistics*, 248–264. Dubrovnik, Croatia: Association for Computational Linguistics.

- Heimersheim, S.; and Nanda, N. 2024. How to use and interpret activation patching. arXiv:2404.15255.
- Holyoak, K. J.; and Morrison, R. G. 2005. *The Cambridge handbook of thinking and reasoning*. Cambridge University Press. ISBN 0521824176.
- Jason, W.; Yi, T.; Rishi, B.; Colin, R.; Barret, Z.; Sebastian, B.; Dani, Y.; Maarten, B.; Denny, Z.; Donald, M.; Ed, H. C.; Tatsunori, H.; Oriol, V.; Percy, L.; Jeff, D.; and William, F. 2022. Emergent Abilities of Large Language Models. *Transactions on Machine Learning Research*.
- Kaplan, J.; McCandlish, S.; Henighan, T.; Brown, T. B.; Chess, B.; Child, R.; Gray, S.; Radford, A.; Wu, J.; and Amodei, D. 2020. Scaling laws for neural language models. *arXiv preprint arXiv:2001.08361*.
- Kassner, N.; Krojer, B.; and Schütze, H. 2020. Are Pre-trained Language Models Symbolic Reasoners over Knowledge? In Fernández, R.; and Linzen, T., eds., *Proceedings of the 24th Conference on Computational Natural Language Learning*, 552–564. Online: Association for Computational Linguistics.
- Kojima, T.; Gu, S. S.; Reid, M.; Matsuo, Y.; and Iwasawa, Y. 2022. Large Language Models are Zero-Shot Reasoners. In Koyejo, S.; Mohamed, S.; Agarwal, A.; Belgrave, D.; Cho, K.; and Oh, A., eds., *Advances in Neural Information Processing Systems*, volume 35, 22199–22213. Curran Associates, Inc.
- MacCartney, B.; and Manning, C. D. 2007. Natural Logic for Textual Inference. In Sekine, S.; Inui, K.; Dagan, I.; Dolan, B.; Giampiccolo, D.; and Magnini, B., eds., *Proceedings of the ACL-PASCAL Workshop on Textual Entailment and Paraphrasing*, 193–200. Prague: Association for Computational Linguistics.
- Meng, K.; Bau, D.; Andonian, A. J.; and Belinkov, Y. 2022. Locating and Editing Factual Associations in GPT. In Oh, A. H.; Agarwal, A.; Belgrave, D.; and Cho, K., eds., *Advances in Neural Information Processing Systems*.
- Monea, G.; Peyrard, M.; Josifoski, M.; Chaudhary, V.; Eisner, J.; Kiciman, E.; Palangi, H.; Patra, B.; and West, R. 2024. A Glitch in the Matrix? Locating and Detecting Language Model Grounding with Fakepedia. In Ku, L.-W.; Martins, A.; and Srikumar, V., eds., *Proceedings of the 62nd Annual Meeting of the Association for Computational Linguistics (Volume 1: Long Papers)*, 6828–6844. Bangkok, Thailand: Association for Computational Linguistics.
- Nanda, N.; and Bloom, J. 2022. TransformerLens. <https://github.com/TransformerLensOrg/TransformerLens>.
- Nanda, N.; Chan, L.; Lieberum, T.; Smith, J.; and Steinhardt, J. 2023. Progress measures for grokking via mechanistic interpretability. In *The Eleventh International Conference on Learning Representations*.
- Nostalgebraist. 2020. Interpreting GPT: The logit lens. <https://www.lesswrong.com/posts/AcKRB8wDpdaN6v6ru/interpreting-gpt-the-logit-lens>. Accessed: 2024-08-11.
- Olah, C.; Cammarata, N.; Schubert, L.; Goh, G.; Petrov, M.; and Carter, S. 2020. Zoom in: An introduction to circuits. *Distill*, 5(3): e00024. 001.
- Olsson, C.; Elhage, N.; Nanda, N.; Joseph, N.; DasSarma, N.; Henighan, T.; Mann, B.; Askell, A.; Bai, Y.; Chen, A.; Conerly, T.; Drain, D.; Ganguli, D.; Hatfield-Dodds, Z.; Hernandez, D.; Johnston, S.; Jones, A.; Kernion, J.; Lovitt, L.; Ndousse, K.; Amodei, D.; Brown, T.; Clark, J.; Kaplan, J.; McCandlish, S.; and Olah, C. 2022. In-context Learning and Induction Heads. *Transformer Circuits Thread*. <https://transformer-circuits.pub/2022/in-context-learning-and-induction-heads/index.html>.
- OpenAI; Achiam, J.; Adler, S.; Agarwal, S.; Ahmad, L.; Akkaya, I.; Aleman, F. L.; Almeida, D.; Altenschmidt, J.; Altman, S.; Anadkat, S.; Avila, R.; Babuschkin, I.; Balaji, S.; Balcom, V.; Baltescu, P.; Bao, H.; Bavarian, M.; Belgum, J.; Bello, I.; Berdine, J.; Bernadett-Shapiro, G.; Berner, C.; Bogdonoff, L.; Boiko, O.; Boyd, M.; Brakman, A.-L.; Brockman, G.; Brooks, T.; Brundage, M.; Button, K.; Cai, T.; Campbell, R.; Cann, A.; Carey, B.; Carlson, C.; Carmichael, R.; Chan, B.; Chang, C.; Chantzis, F.; Chen, D.; Chen, S.; Chen, R.; Chen, J.; Chen, M.; Chess, B.; Cho, C.; Chu, C.; Chung, H. W.; Cummings, D.; Currier, J.; Dai, Y.; Decareaux, C.; Degry, T.; Deutsch, N.; Deville, D.; Dhar, A.; Dohan, D.; Dowling, S.; Dunning, S.; Ecoffet, A.; Eleti, A.; Eloundou, T.; Farhi, D.; Fedus, L.; Felix, N.; Fishman, S. P.; Forte, J.; Fulford, I.; Gao, L.; Georges, E.; Gibson, C.; Goel, V.; Gogineni, T.; Goh, G.; Gontijo-Lopes, R.; Gordon, J.; Grafstein, M.; Gray, S.; Greene, R.; Gross, J.; Gu, S. S.; Guo, Y.; Hallacy, C.; Han, J.; Harris, J.; He, Y.; Heaton, M.; Heidecke, J.; Hesse, C.; Hickey, A.; Hickey, W.; Hoeschele, P.; Houghton, B.; Hsu, K.; Hu, S.; Hu, X.; Huizinga, J.; Jain, S.; Jain, S.; Jang, J.; Jiang, A.; Jiang, R.; Jin, H.; Jin, D.; Jomoto, S.; Jonn, B.; Jun, H.; Kafkhan, T.; Łukasz Kaiser; Kamali, A.; Kanitscheider, I.; Keskar, N. S.; Khan, T.; Kilpatrick, L.; Kim, J. W.; Kim, C.; Kim, Y.; Kirchner, J. H.; Kiros, J.; Knight, M.; Kokotajlo, D.; Łukasz Kondraciuk; Kondrich, A.; Konstantinidis, A.; Kosic, K.; Krueger, G.; Kuo, V.; Lampe, M.; Lan, I.; Lee, T.; Leike, J.; Leung, J.; Levy, D.; Li, C. M.; Lim, R.; Lin, M.; Lin, S.; Litwin, M.; Lopez, T.; Lowe, R.; Lue, P.; Makanju, A.; Malfacini, K.; Manning, S.; Markov, T.; Markovski, Y.; Martin, B.; Mayer, K.; Mayne, A.; McGrew, B.; McKinney, S. M.; McLeavey, C.; McMillan, P.; McNeil, J.; Medina, D.; Mehta, A.; Menick, J.; Metz, L.; Mishchenko, A.; Mishkin, P.; Monaco, V.; Morikawa, E.; Mossing, D.; Mu, T.; Murati, M.; Murk, O.; Mély, D.; Nair, A.; Nakano, R.; Nayak, R.; Neelakantan, A.; Ngo, R.; Noh, H.; Ouyang, L.; O’Keefe, C.; Pachocki, J.; Paino, A.; Palermio, J.; Pantuliano, A.; Parascandolo, G.; Parish, J.; Parparita, E.; Passos, A.; Pavlov, M.; Peng, A.; Perelman, A.; de Avila Belbute Peres, F.; Petrov, M.; de Oliveira Pinto, H. P.; Michael; Pokorny; Pokrass, M.; Pong, V. H.; Powell, T.; Power, A.; Power, B.; Proehl, E.; Puri, R.; Radford, A.; Rae, J.; Ramesh, A.; Raymond, C.; Real, F.; Rimbach, K.; Ross, C.; Rotsted, B.; Roussez, H.; Ryder, N.; Saltarelli, M.; Sanders, T.; Santurkar, S.; Sastry, G.; Schmidt, H.; Schnurr, D.; Schulman, J.; Selman, D.; Sheppard, K.; Sherbakov, T.; Shieh, J.; Shoker, S.; Shyam, P.; Sidor, S.; Sigler, E.; Simens, M.; Sitkin, J.; Slama, K.; Sohl, I.; Sokolowsky, B.; Song, Y.; Staudacher, N.; Such, F. P.; Summers, N.; Sutskever, I.; Tang, J.; Tezak, N.; Thompson, M. B.; Tillet, P.; Tootoonchian, A.; Tseng,

- E.; Tuggle, P.; Turley, N.; Tworek, J.; Uribe, J. F. C.; Valone, A.; Vijayvergiya, A.; Voss, C.; Wainwright, C.; Wang, J. J.; Wang, A.; Wang, B.; Ward, J.; Wei, J.; Weinmann, C.; Welihinda, A.; Welinder, P.; Weng, J.; Weng, L.; Wiethoff, M.; Willner, D.; Winter, C.; Wolrich, S.; Wong, H.; Workman, L.; Wu, S.; Wu, J.; Wu, M.; Xiao, K.; Xu, T.; Yoo, S.; Yu, K.; Yuan, Q.; Zaremba, W.; Zellers, R.; Zhang, C.; Zhang, M.; Zhao, S.; Zheng, T.; Zhuang, J.; Zhuk, W.; and Zoph, B. 2024. GPT-4 Technical Report. arXiv:2303.08774.
- Quirke, P.; and Barez, F. 2024. Understanding Addition in Transformers. In *The Twelfth International Conference on Learning Representations*.
- Radford, A.; Narasimhan, K.; Salimans, T.; and Sutskever, I. 2018. Improving Language Understanding by Generative Pre-Training. *OpenAI blog*.
- Radford, A.; Wu, J.; Child, R.; Luan, D.; Amodei, D.; and Sutskever, I. 2019. Language models are unsupervised multitask learners. *OpenAI blog*.
- Rae, J. W.; Borgeaud, S.; Cai, T.; Millican, K.; Hoffmann, J.; Song, F.; Aslanides, J.; Henderson, S.; Ring, R.; Young, S.; Rutherford, E.; Hennigan, T.; Menick, J.; Cassirer, A.; Powell, R.; van den Driessche, G.; Hendricks, L. A.; Rauh, M.; Huang, P.-S.; Glaese, A.; Welbl, J.; Dhathathri, S.; Huang, S.; Uesato, J.; Mellor, J.; Higgins, I.; Creswell, A.; McAleese, N.; Wu, A.; Elsen, E.; Jayakumar, S.; Buchatskaya, E.; Budden, D.; Sutherland, E.; Simonyan, K.; Paganini, M.; Sifre, L.; Martens, L.; Li, X. L.; Kuncoro, A.; Nematzadeh, A.; Gribovskaya, E.; Donato, D.; Lazaridou, A.; Mensch, A.; Lespiau, J.-B.; Tsimpoukelli, M.; Grigorev, N.; Fritz, D.; Sottiaux, T.; Pajarskas, M.; Pohlen, T.; Gong, Z.; Toyama, D.; de Masson d’Autume, C.; Li, Y.; Terzi, T.; Mikulik, V.; Babuschkin, I.; Clark, A.; de Las Casas, D.; Guy, A.; Jones, C.; Bradbury, J.; Johnson, M.; Hechtman, B.; Weidinger, L.; Gabriel, I.; Isaac, W.; Lockhart, E.; Osindero, S.; Rimell, L.; Dyer, C.; Vinyals, O.; Ayoub, K.; Stanway, J.; Bennett, L.; Hassabis, D.; Kavukcuoglu, K.; and Irving, G. 2022. Scaling Language Models: Methods, Analysis & Insights from Training Gopher. arXiv:2112.11446.
- Rozanova, J.; Ferreira, D.; Thayaparan, M.; Valentino, M.; and Freitas, A. 2022. Decomposing Natural Logic Inferences for Neural NLI. In Bastings, J.; Belinkov, Y.; Elazar, Y.; Hupkes, D.; Saphra, N.; and Wiegrefe, S., eds., *Proceedings of the Fifth BlackboxNLP Workshop on Analyzing and Interpreting Neural Networks for NLP*, 394–403. Abu Dhabi, United Arab Emirates (Hybrid): Association for Computational Linguistics.
- Rozanova, J.; Valentino, M.; Cordeiro, L.; and Freitas, A. 2023. Interventional Probing in High Dimensions: An NLI Case Study. In Vlachos, A.; and Augenstein, I., eds., *Findings of the Association for Computational Linguistics: EACL 2023*, 2489–2500. Dubrovnik, Croatia: Association for Computational Linguistics.
- Rozanova, J.; Valentino, M.; and Freitas, A. 2024. Estimating the Causal Effects of Natural Logic Features in Transformer-Based NLI Models. In Calzolari, N.; Kan, M.-Y.; Hoste, V.; Lenci, A.; Sakti, S.; and Xue, N., eds., *Proceedings of the 2024 Joint International Conference on Computational Linguistics, Language Resources and Evaluation (LREC-COLING 2024)*, 6319–6329. Torino, Italia: ELRA and ICCL.
- Simoulin, A.; and Crabbé, B. 2021. How many layers and why? An analysis of the model depth in transformers. In *Proceedings of the 59th Annual Meeting of the Association for Computational Linguistics and the 11th International Joint Conference on Natural Language Processing: Student Research Workshop*, 221–228.
- Stolfo, A.; Belinkov, Y.; and Sachan, M. 2023. A Mechanistic Interpretation of Arithmetic Reasoning in Language Models using Causal Mediation Analysis. In *The 2023 Conference on Empirical Methods in Natural Language Processing*.
- Talmor, A.; Elazar, Y.; Goldberg, Y.; and Berant, J. 2020. oLMpics-On What Language Model Pre-training Captures. *Transactions of the Association for Computational Linguistics*, 8: 743–758.
- Vig, J.; Gehrmann, S.; Belinkov, Y.; Qian, S.; Nevo, D.; Singer, Y.; and Shieber, S. 2020. Investigating Gender Bias in Language Models Using Causal Mediation Analysis. In Larochelle, H.; Ranzato, M.; Hadsell, R.; Balcan, M.; and Lin, H., eds., *Advances in Neural Information Processing Systems*, volume 33, 12388–12401. Curran Associates, Inc.
- Wallat, J.; Singh, J.; and Anand, A. 2020. BERTnesia: Investigating the capture and forgetting of knowledge in BERT. In Alishahi, A.; Belinkov, Y.; Chrupała, G.; Hupkes, D.; Pinter, Y.; and Sajjad, H., eds., *Proceedings of the Third BlackboxNLP Workshop on Analyzing and Interpreting Neural Networks for NLP*, 174–183. Online: Association for Computational Linguistics.
- Wang, K. R.; Variengien, A.; Conmy, A.; Shlegeris, B.; and Steinhardt, J. 2023. Interpretability in the Wild: a Circuit for Indirect Object Identification in GPT-2 Small. In *The Eleventh International Conference on Learning Representations*.
- Wang, Z.; Wang, Y.; Zhang, Z.; Zhou, Z.; Jin, H.; Hu, T.; Sun, J.; Li, Z.; Zhang, Y.; and Xu, Z.-Q. J. 2024. Towards understanding how transformer perform multi-step reasoning with matching operation. *arXiv preprint arXiv:2405.15302*.
- Wei, J.; Wang, X.; Schuurmans, D.; Bosma, M.; brian ichter; Xia, F.; Chi, E. H.; Le, Q. V.; and Zhou, D. 2022. Chain of Thought Prompting Elicits Reasoning in Large Language Models. In Oh, A. H.; Agarwal, A.; Belgrave, D.; and Cho, K., eds., *Advances in Neural Information Processing Systems*.
- Wiegrefe, S.; Tafjord, O.; Belinkov, Y.; Hajishirzi, H.; and Sabharwal, A. 2024. Answer, Assemble, Ace: Understanding How Transformers Answer Multiple Choice Questions. arXiv:2407.15018.
- Wu, Y.; Han, M.; Zhu, Y.; Li, L.; Zhang, X.; Lai, R.; Li, X.; Ren, Y.; Dou, Z.; and Cao, Z. 2023. Hence, Socrates is mortal: A Benchmark for Natural Language Syllogistic Reasoning. In Rogers, A.; Boyd-Graber, J.; and Okazaki, N., eds., *Findings of the Association for Computational Linguistics: ACL 2023*, 2347–2367. Toronto, Canada: Association for Computational Linguistics.

Wu, Z.; Qiu, L.; Ross, A.; Akyürek, E.; Chen, B.; Wang, B.; Kim, N.; Andreas, J.; and Kim, Y. 2024. Reasoning or Reciting? Exploring the Capabilities and Limitations of Language Models Through Counterfactual Tasks. In Duh, K.; Gomez, H.; and Bethard, S., eds., *Proceedings of the 2024 Conference of the North American Chapter of the Association for Computational Linguistics: Human Language Technologies (Volume 1: Long Papers)*, 1819–1862. Mexico City, Mexico: Association for Computational Linguistics.

Yu, Q.; Merullo, J.; and Pavlick, E. 2023. Characterizing Mechanisms for Factual Recall in Language Models. In Bouamor, H.; Pino, J.; and Bali, K., eds., *Proceedings of the 2023 Conference on Empirical Methods in Natural Language Processing*, 9924–9959. Singapore: Association for Computational Linguistics.

Appendix

This document serves as a technical appendix to the paper titled *A Mechanistic Interpretation of Syllogistic Reasoning in Auto-Regressive Language Models*. It provides additional theoretical background, experimental details, and supplementary results that support the main findings presented in the original paper.

A. Unconditionally Valid Syllogism Schemes

We list all 15 unconditionally valid syllogisms (Table 3).

B. Dataset Generation

B.1. Symbolic

The symbolic dataset comprises sentences where all terms in the premises are represented by abstract symbols (uppercase alphabet letters). From the set of all 26 uppercase alphabets, three-letter triples (e.g., A, B and C) are randomly sampled. For each triple, six permuted prompts and label pairs are generated following a template designed to minimise latent semantic interference among alphabet symbol tokens.

B.2. Non-symbolic

The non-symbolic datasets are constructed based on GenericsKB (Bhaktavatsalam, Anastasiades, and Clark 2020), a resource that provides a foundation for evaluation of sentence veracity with associated truthfulness scores (0-1). The dataset construction process involves the following steps:

- **Extraction:** Select generic sentences with a truthfulness score of 1 based on GenericsKB (Bhaktavatsalam, Anastasiades, and Clark 2020), specifically those in the form *A are B*, using regular expression.
- **Syllogism Construction:** We form universal affirmative syllogism arguments (*Barbara*) based on a template by chaining sentences where the predicate of one sentence logically matches the subject of another.
- **Constraints:** We exclude terms tokenised into multiple tokens to maintain consistency in comparison with the symbolic dataset, which is essential for coherent circuit analysis.

- **Classification:** To address issues of partial inclusion and syntactic ambiguity in constructed syllogism arguments, we employ GPT-4 (OpenAI et al. 2024) to classify whether arguments contain only truthful premises and whether the middle-terms are syntactically and semantically equivalent. This step helps us classify a belief-consistent dataset and a belief-inconsistent dataset.
- **Validation:** We manually evaluate the alignment of classified arguments with human belief-consistency (i.e., premises are true and logic is valid).

This process ensures that our non-symbolic dataset maintains logical equivalence with the symbolic dataset while incorporating meaningful semantic real-word concepts.

B.3. Data Statistics

We organise data statistics for generated datasets (Table 4).

C. Embedding Space Analysis Details

One well-known method for analysing hidden activation in transformer language models is projecting activation into embedding space, the so-called logit lens (Nostalgebraist 2020; Elhage et al. 2021; Geva et al. 2022). In particular, we focus on an input-agnostic approach (Dar et al. 2023; Hanna, Liu, and Variengien 2024), utilising both unembedding (\mathbf{W}_U) and embedding (\mathbf{W}_E) matrices to construct a $\mathbb{R}^{|V| \times |V|}$ matrix, where $|V|$ represents the model’s vocabulary size. In this study, we employ the OV circuit (Elhage et al. 2021) of attention heads, formed by attention value and output weights ($W_V W_O$), to understand the general behaviour of how source tokens influence output logits. The OV circuit-based logit lens for attention head \mathbf{h} is formalised as $\mathbf{W}_E \mathbf{W}_V^h \mathbf{W}_O^h \mathbf{W}_U \in \mathbb{R}^{|V| \times |V|}$. For simplicity and in line with established conventions (Elhage et al. 2021; Dar et al. 2023), this formulation ignores layer normalisation.

D. Circuit Ablation Method Details

To measure the necessity and sufficiency of the circuit \mathcal{C} in the model \mathcal{M} , we knock out attention heads in \mathcal{H} from the model \mathcal{M} and measure the average logit difference $\delta(p, m)$ along the batch. We denote the logit difference in circuit state \mathcal{C} as $\delta(p, m, \mathcal{C})$ and every subset of heads set as $H \subset \mathcal{H}$.

In order to verify the head’s necessity in the model, we conduct a cumulative ablation of \mathcal{C} from total circuit \mathcal{M} , progressing from downstream to upstream layers. At each ablation step k , where $\mathcal{C}_k^* = \mathcal{M} \setminus H_k$ and H_k denotes the set of ablated attention heads up to step k as:

$$\mathbb{E}_{x \sim X} [\delta_k(p, m, \mathcal{C}_k^*)] \quad \text{where} \quad \mathcal{C}_k^* = \mathcal{M} \setminus H_k$$

Conversely, we perform a cumulative addition of attention heads for evaluating the sufficiency of the circuit, starting from earlier layers and progressing to later ones, while maintaining all other attention heads in a mean-ablated state. At each addition step j , where $\mathcal{C}_j^* = \mathcal{M} \setminus (\mathcal{H} \setminus H_j)$ and H_j denotes the set of added attention heads up to step j as:

$$\mathbb{E}_{x \sim X} [\delta_j(p, m, \mathcal{C}_j^*)] \quad \text{where} \quad \mathcal{C}_j^* = \mathcal{M} \setminus (\mathcal{H} \setminus H_j)$$

Name	Mood	Figure	Premise (m)	Premise (M)	Conclusion
Barbara	AAA	1	$\forall x(s, m)$ <i>All A are B.</i>	$\forall x(m, p)$ <i>All B are C.</i>	$\forall x(s, p)$ <i>All A are C.</i>
Celarent	EAE	1	$\forall x(s, m)$ <i>All A are B.</i>	$\forall x\neg(m, p)$ <i>No B are C.</i>	$\forall x\neg(s, p)$ <i>No A are C.</i>
Darii	AII	1	$\exists x(s, m)$ <i>Some A are B.</i>	$\forall x(m, p)$ <i>All B are C.</i>	$\exists x(s, p)$ <i>Some A are C.</i>
Ferio	EIO	1	$\exists x(s, m)$ <i>Some A are B.</i>	$\forall x\neg(m, p)$ <i>No B are C.</i>	$\exists x\neg(s, p)$ <i>Some A are not C.</i>
Camestres	AEE	2	$\forall x\neg(s, m)$ <i>No A are B.</i>	$\forall x(p, m)$ <i>All C are B.</i>	$\forall x\neg(s, p)$ <i>No A are C.</i>
Cesare	EAE	2	$\forall x(s, m)$ <i>All A are B.</i>	$\forall x\neg(p, m)$ <i>No C are B.</i>	$\forall x\neg(s, p)$ <i>No A are C.</i>
Baroco	AOO	2	$\exists x\neg(s, m)$ <i>Some A are not B.</i>	$\forall x(p, m)$ <i>All C are B.</i>	$\exists x(s, p)$ <i>Some A are not C.</i>
Festino	EIO	2	$\exists x(s, m)$ <i>Some A are B.</i>	$\forall x\neg(p, m)$ <i>No C are B.</i>	$\exists x\neg(s, p)$ <i>Some A are not C.</i>
Disamis	IAI	3	$\forall x(m, s)$ <i>All B are A.</i>	$\exists x(m, p)$ <i>Some B are C.</i>	$\exists x(s, p)$ <i>Some A are C.</i>
Datisi	AII	3	$\exists x(m, s)$ <i>Some B are A.</i>	$\forall x(m, p)$ <i>All B are C.</i>	$\exists x(s, p)$ <i>Some A are C.</i>
Ferison	EIO	3	$\exists x(m, s)$ <i>Some B are A.</i>	$\forall x\neg(m, p)$ <i>No B are C.</i>	$\exists x\neg(s, p)$ <i>Some A are not C.</i>
Bokardo	OAO	3	$\forall x(m, s)$ <i>All B are A.</i>	$\exists x\neg(m, p)$ <i>Some B are not C.</i>	$\exists x\neg(s, p)$ <i>Some A are not C.</i>
Dimaris	IAI	4	$\forall x(m, s)$ <i>All B are A.</i>	$\exists x(p, m)$ <i>Some C are B.</i>	$\exists x(s, p)$ <i>Some A are C.</i>
Camenes	AEE	4	$\forall x\neg(m, s)$ <i>No B are A.</i>	$\forall x(p, m)$ <i>All C are B.</i>	$\forall x\neg(s, p)$ <i>No A are C.</i>
Fresison	EIO	4	$\exists x(m, s)$ <i>Some B are A.</i>	$\forall x\neg(p, m)$ <i>No C are B.</i>	$\exists x\neg(s, p)$ <i>Some A are not C.</i>

Table 3: 15 Unconditionally valid syllogisms schemes. The table lists the syllogisms by their traditional names, moods, and figures, with formalised logical expressions on the first line and corresponding natural language examples on the second line. The minor premise (m) is presented before the major premise (M) to emphasise the transitive property inherent in these forms.

Statistic	SYM	BC	BI
Number of Samples	90	90	90
Token Sequence Length	15	15	15
Unique Terms (s)	26	87	86
Unique Terms (m)	26	70	35
Unique Terms (p)	26	59	64

Table 4: Summary of Dataset Statistics. **SYM** refers to the symbolic dataset, **BC** refers to the non-symbolic belief-consistent dataset, and **BI** refers to the non-symbolic belief-inconsistent dataset.

E. GPT-2 Model Architecture

We provide a self-contained concise overview of the GPT-2 model architecture, highlighting the main components and their mathematical relationships. Bias terms are not presented for the simplicity. We refer the conventions of notation in Elhage et al. (2021) and (Geva et al. 2023).

Notation and Preliminaries

- x_i - One-hot encoded vector representing the i -th token in the input sequence.
- $W_E^{\text{token}}, W_E^{\text{pos}}$ - Token and positional embedding matrices.
- W_Q, W_K, W_V - Query, key, and value weight matrices of attention heads.
- $W^{\text{in}}, W^{\text{out}}$ - Input and output weight matrices of MLP feed-forward networks.
- d - Dimension of the attention head state embedding vectors.
- D - Dimension of the hidden state embedding vectors.
- N - Length of the input sequence.
- L - Total number of transformer layers.
- \mathcal{V} - Vocabulary set of the model.
- σ and σ' - Activation functions used in self-attention and MLP sublayers, respectively.

Embedding Layer. Each token in the input sequence is transformed into an embedded representation by combining token-specific and positional embeddings:

$$r_i^0 = x_i W_E^{\text{token}} + x_i W_E^{\text{pos}}$$

This operation initializes the input for the transformer layers, where r_i^0 represents the initial embedded state of the i -th token.

Residual Stream. The residual stream facilitates the propagation of information across transformer layers. It is updated at each layer by contributions from the multi-head self-attention and multi-layer perceptron sublayers:

$$r_i^l = r_i^{l-1} + A_i^l + M_i^l$$

where r_i^l represents the state of the i -th token at layer l , and A_i^l, M_i^l are outputs from the Multi-Head Self-Attention (MHSA) and Multi-Layer Perceptron (MLP) sublayers.

Multi-Head Self-Attention (MHSA). This sublayer processes information by applying self-attention mechanisms across multiple ‘heads’ of attention, enabling the model to capture various aspects of the input data, where σ represent the non-linearity function:

$$A_i^l = \sum_{h \in H} \left(\sigma \left(\frac{(r_i^{l,h} W_Q^h)(r_i^{l,h} W_K^h)^T}{\sqrt{d_K}} \right) (r_i^{l,h} W_V^h) \right) W_O^h$$

Each head computes a weighted sum of all tokens’ transformed states, focusing on different subsets of sequence information.

Multi-Layer Perceptron (MLP). Each token’s representation is further processed in a position-wise manner by the MLP sublayer:

$$M_i^l = \sigma'(r_i^l W^{in})(W^{out})^T$$

The MLP modifies each token’s state locally, enhancing its ability to process information.

Layer Normalisation. Before processing by MHSA and MLP, each token’s state is normalised to stabilise learning and reduce training time:

$$\text{LN}(r_i^l) = \gamma \odot \frac{r_i^l - \mu_i^l}{\sqrt{(\sigma_i^l)^2 + \epsilon}} + \beta$$

This step ensures that the activations across different network layers maintain a consistent scale.

Prediction Head. The prediction head generates logits for the next token prediction using the final transformed states:

$$\text{logits}_N = \text{LN}(r_N^L) W_U$$

The predicted token is chosen based on the sampling method (e.g., greedy decoding) at the last position N .

F. Path Patching Details

Path patching, an generalised version of activation patching, aims to compute direct effects among model components, rather than indirect effects diffused from intervened components (Wang et al. 2023). This method involves freezing non-targeted activations during an initial forward pass, storing the corrupted targeted activation state, and then executing a subsequent forward pass with the targeted activation state substituted by the corrupted one. This approach isolates targeted component-to-component effects, eliminating non-relevant interactions. In our implementation, we employ a noising method where clean activations are replaced with corrupted ones, resulting in negative scores indicating positive contributions from corresponding components. Our findings, illustrated in Figure 7, reveal that $\mathbf{h}_{11.10}$ strongly operates based on several heads: $\mathbf{h}_{5.8}$, $\mathbf{h}_{6.1}$, $\mathbf{h}_{6.15}$, and $\mathbf{h}_{7.2}$. Manual investigation of attention patterns subsequently confirmed these as induction heads (Elhage et al. 2021).

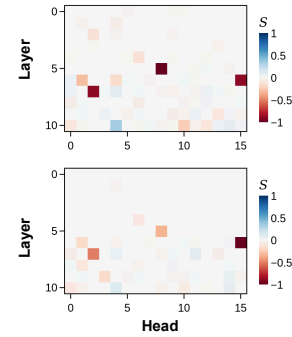


Figure 7: Path patching results for (Top) symbolic inputs and non-symbolic inputs (Bottom) in the middle-term corruption setup. Note that negative heads are positively influencing heads, as we replace corrupted activation with clean ones in our noising approach.

G. Localising Mover Heads

To efficiently classify the numerous attention heads (384 in GPT-2 medium) within the model, we calculate the Positional Patching Difference (PPD) to construct four-quadrant analysis. This method involves intervening in the attention value weights W_V and constructs a distribution layout of heads, providing a systematic classification for quadrant groups. The layout is composed of the PPD score ($|S[p]| - |S[m_1]| + S[m_2]$) on the x-axis and the patching score for all sequence positions (\mathcal{S}) on the y-axis.

Based on this PPD score quadrant layout analysis, we categorise heads according to their quadrant positions, revealing insights into their functional roles:

- (1) First quadrant (Positive Copy Candidates): Heads with $\mathcal{S} > 0$ and positive PPD, predominantly copying $[p]$ -based information.
- (2) Second quadrant (Positive Suppression Candidates): Heads with $\mathcal{S} > 0$ but negative PPD, predominantly suppressing $[m]$ -based information.

- (3) Third quadrant (Negative Copy Candidates): Heads with $\mathcal{S} < 0$ and negative PPD, predominantly copying $[m]$ -based information.
- (4) Fourth quadrant (Negative Suppression Candidates): Heads with $\mathcal{S} < 0$ but positive PPD, predominantly suppressing $[p]$ -based information.

The intervention of attention head values (W_V) is crucial because all-term corruption maintains the same positional alignment for all samples $(s, m_1, m_2, p) \rightarrow (s', m'_1, m'_2, p')$, resulting in minimal impact from attention head pattern interventions composed by attention query and key. Consequently, we can infer that the attention head output patching results primarily derive from the attention value activation. This property enables us to localise the source token positions from which the term information is moved by attention value patching.

Formally, we denote the attention query, key, value, and output matrix activations as \mathbf{W}_Q , \mathbf{W}_K , \mathbf{W}_V , and \mathbf{W}_O respectively. One attention head output can be expressed as $\sigma((\mathbf{R}\mathbf{W}_Q)(\mathbf{R}\mathbf{W}_K)^T)(\mathbf{R}\mathbf{W}_V)\mathbf{W}_O$, where σ represents the non-linearity function (softmax in GPT-2) applied in the attention pattern and \mathbf{R} denotes the residual stream.

To include only influential heads in the circuit, we extracted outlier heads with an absolute patching score exceeding the threshold (τ), defined by the mean and standard deviation of all heads' scores as:

$$\{\mathbf{h} \mid |\mathcal{S}_{\mathbf{h}}| > \tau\} \quad \text{where} \quad \tau = \mu + 2\sigma$$

Our analysis identifies 9 heads for the symbolic circuit, as illustrated by red dots in Figure 8(a). $\mathbf{h}_{14.14}$, $\mathbf{h}_{15.14}$, and $\mathbf{h}_{18.12}$ are classified as positive copy heads, while $\mathbf{h}_{19.1}$ is grouped as a positive suppression head. $\mathbf{h}_{9.9}$, $\mathbf{h}_{11.1}$, $\mathbf{h}_{12.1}$, $\mathbf{h}_{17.2}$, and $\mathbf{h}_{23.10}$ are classified as negative copy heads. It is noteworthy that non-symbolic results reveal a more complex and noisy pattern in the mover localisation process (Figure 8(b)).

H. Non-symbolic Circuit Analysis

We present the results of our non-symbolic circuit analysis (Figure 9).

I. Generalisability to Other Syllogisms

To assess the generalisability of our model, we applied the circuit ablation method to all 15 unconditionally valid syllogisms (Table 3) and the result is shown in Figure 10. Unconditionally valid syllogisms are logical arguments that maintain their validity irrespective of the truth values of their premises. The validity of these syllogisms is determined solely by their logical form, which is characterised by mood and figure combinations. The mood of a syllogism is defined by the arrangement of four proposition types ("All (A)", "No (E)", "Some (I)", "Some ... not (O)") across its two premises and conclusion. Conversely, the figure of a categorical syllogism is determined by the structural arrangement of terms within the constituent sentences. This approach enables the evaluation of syntactic logic in isolation from contextual interference and belief-bias effects.

J. Generalisability Across Model Sizes

To assess the generalisability of our findings across different model capacities, we extended our symbolic circuit analysis to various GPT-2 model sizes. Figure 11 presents the results of this comparative analysis.

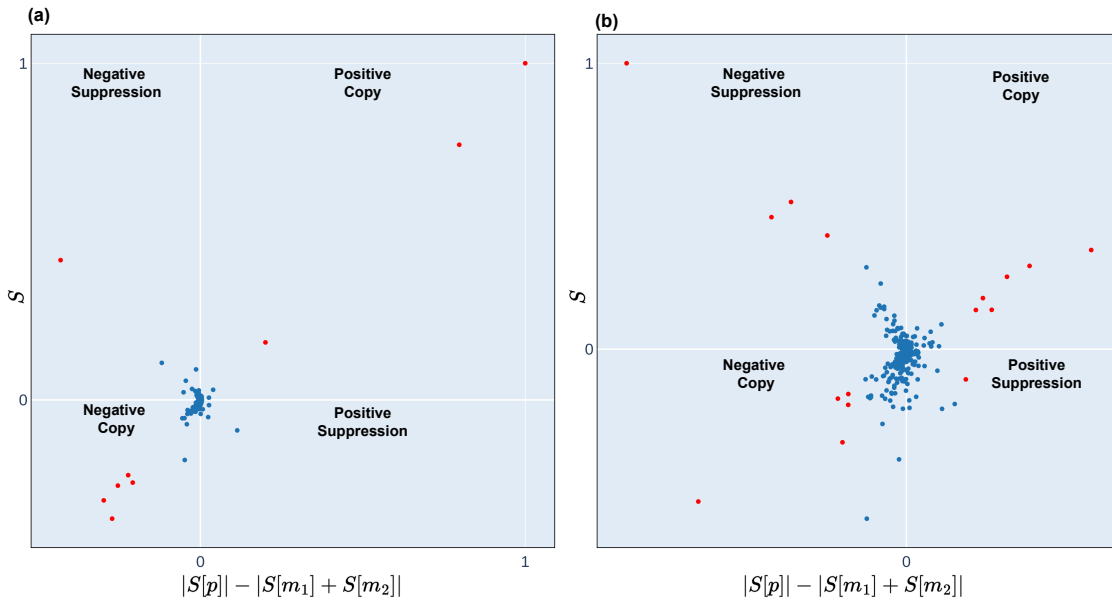


Figure 8: Distribution of attention heads in PPD-based quadrant analysis. (a) Results for symbolic inputs. (b) Results for non-symbolic inputs. The x-axis represents normalised PPD scores, while the y-axis represents normalised attention value-based patching scores (S). Red dots indicate attention heads above the threshold (τ) of patching score.

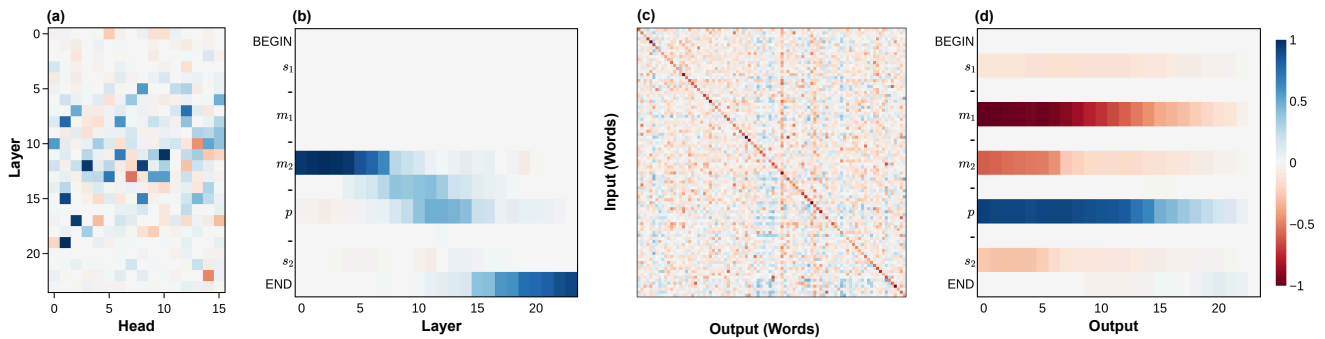


Figure 9: Comprehensive results of the non-symbolic circuit analysis. (a) Attention output patching results and (b) residual stream patching results in the middle-term intervention setup. (c) OV circuit logit lens results for $h_{11.10}$, with input and output comprising 26 uppercase letters. (d) Residual stream patching results in the all-term corruption setup. (e)-(h) Average attention patching weights across the batch: (e) weights for token position $[p]$ attending, and (f)-(h) weights for the last token position attending. For clarity, the y-axis legend denotes tokens appearing between terms, separated by a '-' symbol, with averaged values.

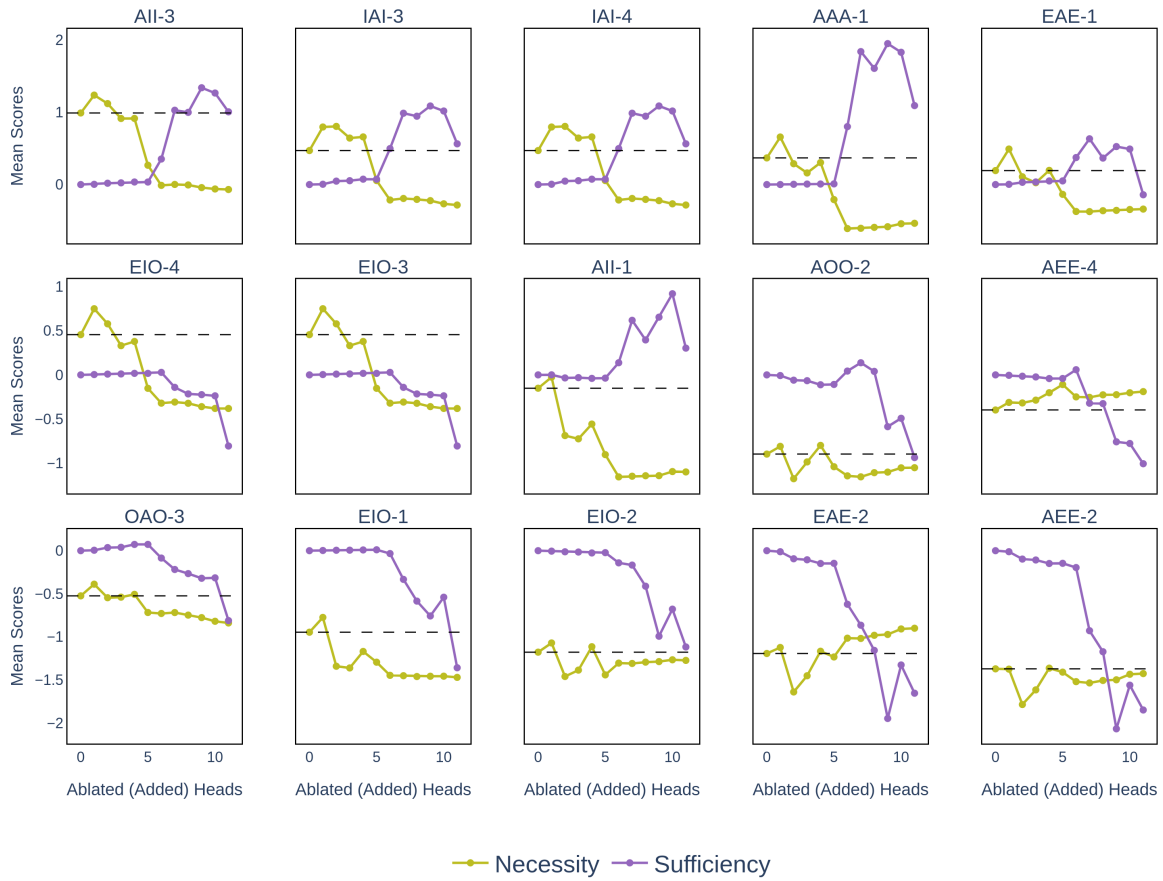


Figure 10: Necessity and sufficiency performance results from circuit ablation method for all unconditionally valid syllogistic forms. Labels (e.g., AII-3) denote mood and figure combinations.

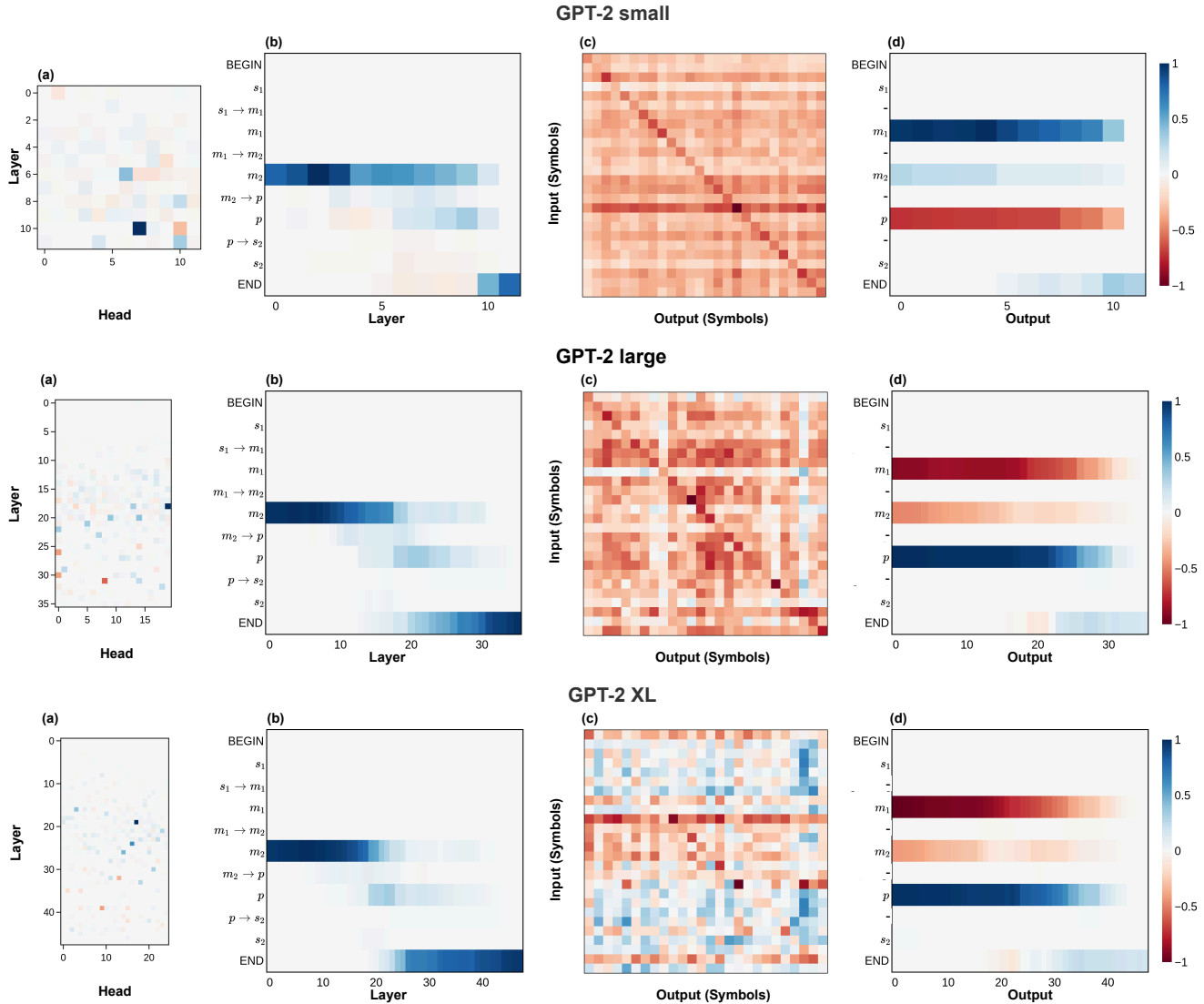


Figure 11: Comprehensive results of the symbolic circuit analysis across different model sizes. (a) Attention output patching results and (b) residual stream patching results in the middle-term intervention setup. (c) OV circuit logit lens results for m -suppression head, with input and output comprising 26 uppercase letters. (d) Residual stream patching results in the all-term corruption setup. For clarity, the y-axis legend denotes tokens appearing between terms, separated by a ‘-’ with averaged values.